A Composite Chiral Pair of Rotational Bands in the Odd-A Nucleus 135Nd

A Composite Chiral Pair of Rotational Bands in the Odd-*A* Nucleus ^{135}Nd

S. Zhu,[1] U. Garg,[1] B. K. Nayak,[1] S. S. Ghugre,[2] N. S. Pattabiraman,[2] D. B. Fossan,[3] T. Koike,[3] K. Starosta,[3] C. Vaman,[3] R. V. F. Janssens,[4] R. S. Chakrawarthy,[5] M. Whitehead,[5] A. O. Macchiavelli,[6] and S. Frauendorf[1]

[1]*Physics Department, University of Notre Dame, Notre Dame, Indiana 46556, USA*
[2]*IUCDAEF-Calcutta Center, Calcutta 700 094, India*
[3]*Department of Physics and Astronomy, State University of New York, Stony Brook, New York 11794, USA*
[4]*Physics Division, Argonne National Laboratory, Argonne, Illinois 60439, USA*
[5]*Schuster Laboratory, University of Manchester, Manchester M13 9PL, United Kingdom*
[6]*Nuclear Physics Division, Lawrence Berkeley National Laboratory, Berkeley, California 94720, USA*

(Received 20 February 2003; revised manuscript received 14 May 2003; published 25 September 2003)

High-spin states in ^{135}Nd were populated with the ^{110}Pd(^{30}Si, $5n$)^{135}Nd reaction at a ^{30}Si bombarding energy of 133 MeV. Two $\Delta I = 1$ bands with close excitation energies and the same parity were observed. These bands are directly linked by $\Delta I = 1$ and $\Delta I = 2$ transitions. The chiral nature of these two bands is confirmed by comparison with three-dimensional tilted axis cranking calculations. This is the first observation of a three-quasiparticle chiral structure and establishes the primarily geometric nature of this phenomenon.

DOI: 10.1103/PhysRevLett.91.132501 PACS numbers: 21.10.Re, 21.60.Ev, 23.20.Lv, 27.60.+j

The rotational motion of triaxial nuclei attains a chiral character if the angular momentum has substantial projections on all three principal axes of the triaxial density distribution [1]. Figure 1 illustrates how chirality emerges from the combination of the triaxial geometry with an axis of rotation that lies out of the three symmetry planes of the ellipsoid. The three components of the angular momentum vector form either a left-handed or a right-handed system. Reversing the direction of the component of the angular momentum on the intermediate axis changes the chirality. The left-handed and right-handed configurations, which have the same energy, manifest themselves as two degenerate rotational bands—the chiral doublet. This argument, which is based only on the symmetry of the rotating triaxial nucleus, is independent of how the three components of the angular momentum are composed [1]. The simplest possibility was considered in Ref. [2] where the concept of chiral rotation was first suggested: one proton aligns its angular momentum with the short axis, one neutron hole aligns its angular momentum with the long axis, and the collective angular momentum generated by all other nucleons aligns with the intermediate axis. Experimental evidence for this simplest type of a chiral configuration was first found in ^{134}Pr [3] and subsequently in a number of other odd-odd nuclei [4–11]. However, chirality is expected for all configurations that have substantial angular momentum components along the three principal axes, no matter how the individual components are composed. In this Letter, we report the first observation of a pair of chiral bands in an odd-*A* nucleus ^{135}Nd. In this case, the angular momentum of two protons is aligned with the short axis and, thus, the chiral bands are based on a three-quasiparticle configuration. Our results represent an important confirmation of the geometrical interpretation in terms of broken chiral symmetry [1] which claims that pairs of nearly degenerate $\Delta I = 1$ bands with the same parity appear whenever there is a chiral geometry of the angular momentum components, irrespective of how they are composed.

High spin states in ^{135}Nd were populated via the ^{110}Pd(^{30}Si, $5n$)^{135}Nd reaction, at a bombarding energy of 133 MeV. The incident beam energy was optimized for this reaction channel by measuring an excitation function. For the purpose, ^{30}Si beams at four different energies from 128 to 143 MeV were obtained in steps of 5 MeV from the FN-tandem injected superconducting LINAC at the State University of New York at Stony Brook. Three Compton-suppressed HPGe detectors were used for γ detection. The beam for the coincidence measurements

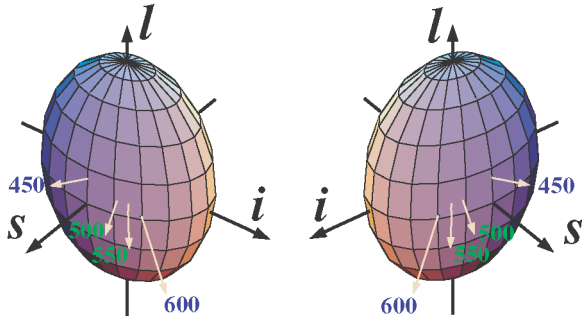

FIG. 1 (color online). The orientation of the total angular momentum vector, $\vec{I}$, with respect to the axes of the triaxially deformed density distribution in ^{135}Nd (light arrows) for different rotational frequencies from the tilted-axis cranking calculations. The numbers show the rotational frequency in keV. The labels *l*, *s*, and *i* stand for long, short, and intermediate axes, respectively. In the order *s*-*i*-*l*, these axes form a "right-handed" system (left part of the figure) and a "left-handed" system (right part of the figure)—a chiral doublet.

was provided by the 88-in. cyclotron facility at the Ernest O. Lawrence Berkeley National Laboratory. Two stacked, self-supporting, isotopically enriched target foils (~ 0.5 mg/cm^2 thick) were used. Quadruple- and higher-fold coincidence events were measured using the Gammasphere array [12] in stand-alone mode, which comprised 103 active Compton-suppressed HPGe detectors. A total of about 1.3×10^9 events were accumulated and stored onto magnetic tapes for further analysis. The data were sorted into three-dimensional (E_γ-E_γ-E_γ cube) and four-dimensional (E_γ-E_γ-E_γ-E_γ hypercube) histograms using the RADWARE formats [13]. These were analyzed with the RADWARE software package, which uses the generalized background subtraction algorithm of Ref. [14], to extract "double-gated" and "triple-gated" spectra. The level scheme was constructed by examination of these gated spectra. The multipolarity assignments were made on the basis of directional correlation of oriented nuclei (DCO) ratios [15] and confirmed by an angular distribution analysis [16].

A partial level scheme for ^{135}Nd, as obtained from the present work, is shown in Fig. 2. The primary feature of interest in the level scheme is a new $\Delta I = 1$ band (band B) which feeds into, and forms a chiral pair with, the structure identified as band A in the yrast sequence. The strong links between the two bands point to their same intrinsic configuration. Figure 3 shows the summed gated coincidence spectra for bands A and B. The spins and parity of the yrast band have been assigned in previous work [17,18]; these agree with the assignments extracted from the aforementioned DCO and angular distribution analyses. The spins in band B have been extracted in exactly the same manner. The $\Delta I = 1$ character of the intraband transitions in band B and of the transitions linking it with band A is also confirmed by angular distribution measurements—typical values of the A_2/A_0 and A_4/A_0 coefficients for these transitions are ~ -0.4 and ~ 0, respectively. In particular, the A_2/A_0 ratios for the 648- and 670-keV linking transitions are $-0.654(30)$ and $-0.564(22)$, respectively, establishing their $\Delta I = 1$ character. To ascertain the mixed $M1/E2$ multipolarity of the intraband transitions, electron conversion (EC) coefficients were estimated from intensity-balance arguments, i.e., by comparing the intensities of the γ rays feeding into and decaying out of the levels involved. For $Z = 60$ and $E_\gamma = 250$ keV, the EC coefficient is ~ 0.2 for an $M1$ transition and ~ 0.02 for an $E1$ transition. The values of the EC coefficients extracted from the data for the 170- and 226-keV transitions are 0.25(10) and 0.17(3), respectively, clearly pointing to their $M1/E2$ character. Looking at the linking transitions, the calculated DCO ratio for an $E1$ transition in our geometry is ~ 0.9, while the measured values for the DCO ratio for the 648- and 670-keV, $\Delta I = 1$ linking transitions are ~ 1.5, pointing to their $M1/E2$ character as well. While it has not been possible to extract angular

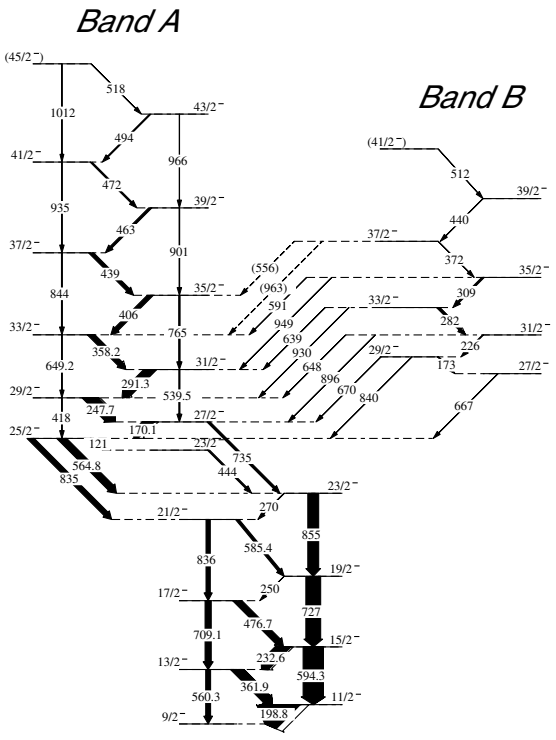

FIG. 2. Partial level scheme showing the $\pi h^2_{11/2} \nu h^{-1}_{11/2}$ band and the newly observed sideband of ^{135}Nd. Bands A and B are interpreted as the chiral pair. The transition intensities are proportional to the thickness of the arrows.

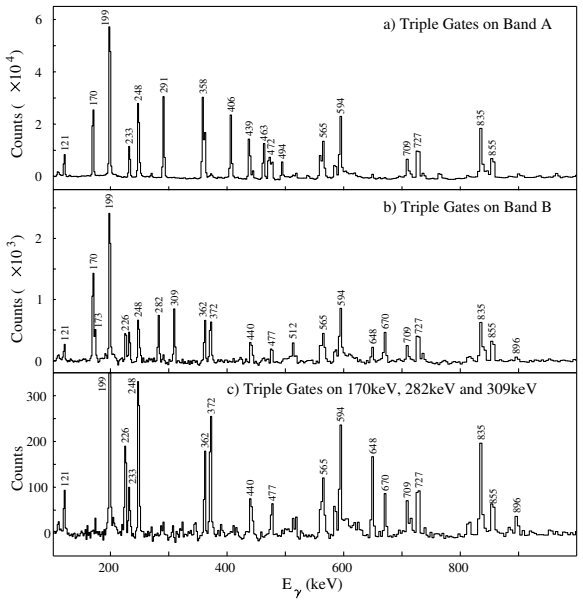

FIG. 3. Background subtracted γ-γ-γ-γ spectra in ^{135}Nd from the summation of spectra with triple gates set on band A (top panel) and B (middle panel). The bottom panel is included to clearly show the presence of the 648-keV ($\Delta I = 1$), 670-keV ($\Delta I = 1$), and 896-keV ($\Delta I = 2$) "linking" transitions in the gated spectra.

distribution ratios for the other linking transitions because of their weak intensities, the ratio of intensity at forward angles to that at 90° for the 896-keV transition is 1.7(3), establishing it as an $E2$ transition. It is evident, therefore, that the two bands have the same parity and are linked by mixed $M1/E2$ and $E2$ transitions.

Three-dimensional tilted axis cranking (3D TAC) calculations have been performed to investigate the possibility of chiral solutions in ^{135}Nd. The TAC model has been discussed in detail in Refs. [19–23]. The deformation parameters ϵ and γ, and the tilt angles θ and ϕ are obtained for a given frequency $\hbar\omega$ and for a given configuration, by searching for a local minimum on the multiparameter surface of the total Routhian. This procedure led to a solution for the $\pi h_{11/2}^2 \nu h_{11/2}^{-1}$ configuration with ϵ and γ values of $\sim$0.20 and $\sim$30°, respectively, for frequencies $\hbar\omega$ between 0.20 and 0.60 MeV. We include the neutron pairing correlations ($\Delta = 1.08$ MeV) but use zero pairing for the proton system, because the pair correlations are blocked by the two $h_{11/2}$ protons. Table I gives detailed results of the calculation and Fig. 1 illustrates how the total angular momentum vector reorients with respect to the deformed density distribution. We note that Piel *et al.* [17] had referred to a stable prolate axial ($\gamma = 0°$) core for this configuration. However, that work entailed standard cranking calculations which are restricted by the assumption that the axis of rotation must coincide with one of the principal axes of the density distribution. Within this restricted variational space, a prolate shape is associated with the energy minimum. The TAC calculations used in the present work are more general and allow for any orientation of the rotational axis. In this framework, the prolate minimum reported by Piel *et al.* is found to be unstable with respect to a tilt of the rotational axis (saddle point) and the true minimum is triaxial and chiral.

The ground band based on $\nu h_{11/2}$ has been studied previously [17,18]. It was suggested that the backbending at $I^\pi = \frac{25^-}{2}$ is due to the alignment of the lowest pair of $h_{11/2}$ protons, thereby giving the configuration $\pi h_{11/2}^2 \nu h_{11/2}^{-1}$. Above the backbend, the yrast band and the new sideband behave as expected from the calculations. At first, the TAC solution is planar ($\phi = 0$). At $\hbar\omega \approx 0.45$ MeV, $I(\omega) \approx 20$, it becomes chiral. The two bands are separated by about 400 keV for $I = \frac{29}{2}$. They approach each other with increasing spin and the energy separation becomes as small as 100 keV at $\hbar\omega \approx 0.45$ MeV, $I \approx 19$, which we interpret as the onset of chirality. This frequency agrees well with the TAC calculation. The change from the planar to the chiral solution is accompanied by a change of the slope of $I(\omega)$. This indicates that, in the chiral regime, the angular momentum increases along the intermediate axis whereas, in the planar regime, it remains in the plane spanned by the short and long axes which have smaller moments of inertia. In our data, band A shows such a change of slope at the expected frequency. However, the corresponding change is not seen in band B (see below for an explanation).

For further interpretation, one has to take into account that TAC gives only the classical orientation, around which $\vec{I}$ executes a quantal motion. In the planar regime ($\phi = 0$), these are slow oscillations of $\vec{I}$ into the left- and right-handed sectors, which are symmetric to the l-s plane; they have been called chiral vibrations [4]. Band A, then, is the zero- and band B the one-phonon state. The frequency of these vibrations decreases with angular momentum until the motion becomes unstable against static chirality. This decrease is reflected as a difference of about 1.5 units of angular momentum in Fig. 4. In the chiral regime, there still remains some tunneling between the left- and right-handed configurations, which causes

TABLE I. Orientation angles θ, ϕ, values $I(\omega)$ of the angular momentum, and the rotational frequencies for the configuration $[\pi h_{11/2}^2, \nu h_{11/2}^{-1}]$ in $^{135}_{60}$Nd from the 3D TAC calculations described in the text. Chiral solutions correspond to both $\theta \neq 0°$ and 90° and $\phi \neq 0°$ and 90°. The angles θ and ϕ are defined with respect to the l and s axes, respectively (see Fig. 1).

$\hbar\omega$ (MeV)	θ	ϕ	$I(\omega)$ [$\hbar$]
0.20	60	0	16.5
0.25	65	0	17.4
0.30	65	0	18.1
0.35	65	0	18.8
0.40	65	0	19.5
0.45	65	0	20.1
0.50	75	±28	22.0
0.55	75	±37	25.0
0.60	85	±47	30.4

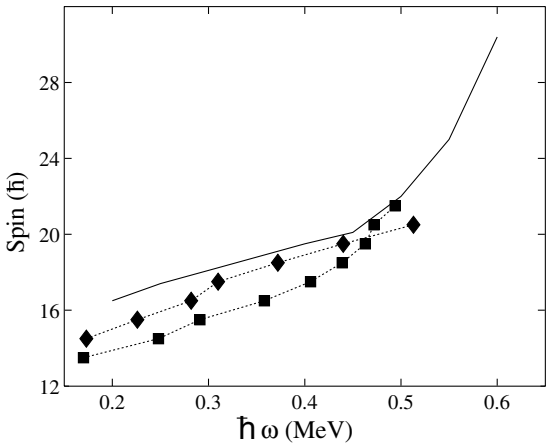

FIG. 4. The experimental spins versus $\hbar\omega$ plots for band A (squares) and band B (diamonds). The solid line is the result of 3D TAC calculations. The dashed lines are to guide the eye.

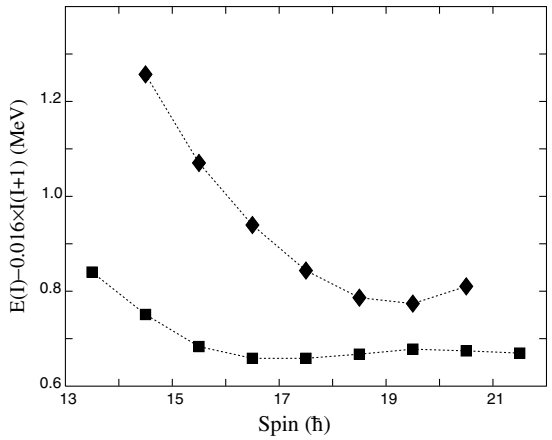

FIG. 5. Experimental excitation energies versus spin for band A (squares) and band B (diamonds). A rigid rotor reference has been subtracted from the energies. The dashed lines are to guide the eye.

the remaining energy difference of about 100 keV between the bands.

The energy difference between the $\frac{41}{2}$ states is slightly larger than for the adjacent lower-spin states as shown in Fig. 5. Such an increase of the splitting is expected from our TAC calculations. As seen in Fig. 1 and Table I, $\vec{I}(\omega)$ approaches the s-i plane for $\hbar\omega > 0.55$ MeV, which means that the tunneling between the left- and right-handed sectors through the s-i plane increases and so does the splitting. For $\hbar\omega = 0.6$ MeV, the TAC solution is almost planar and one is back in the regime of chiral vibrations. Static chirality is, thus, a transient phenomenon, which appears only in a short interval around $I = 19$. The increase of the splitting at high spin may be the reason why the expected up bend of the function $I(\omega)$ is not seen in the upper band—the highest-spin levels in band B are progressively pushed higher in energy compared to those in band A, shifting the data points for these levels in band B to the right in Fig. 4.

Interestingly, a candidate for chiral-doublet bands has recently been proposed in the even-even nucleus ^{136}Nd as well [24]; the suggested configuration was $[\pi(h_{11/2}, d_{5/2}/g_{7/2}), \nu(h^2_{11/2})]$. However, in contrast with the case reported here, and with all odd-odd neighboring nuclei where chiral bands have so far been observed, the bands reported in ^{136}Nd are closest to each other in energy at the lowest spins, with the energy-separation increasing monotonically with increasing spin. It is possible that the reported band-pair originates from a proton pseudospin doublet in the configuration $[\pi(g_{7/2}/g_{9/2}, h_{11/2}), \nu(h^2_{11/2})]$. Indeed, the energy differences are similar to a pair of bands reported recently in ^{128}Pr [25], where such an interpretation has been put forward.

In summary, chiral twin bands based on three quasiparticles have been observed for the first time in this experiment. 3D TAC calculations reproduce the experimental results well, confirming the underlying structure of these bands. As a general property, when angular momentum components align with the three principal axes in a γ-deformed system, chirality manifests itself not only in the odd-odd systems, but also in odd-A systems. The present results establish the primarily geometric character of this phenomenon.

This work has been supported in part by the U.S. National Science Foundation (Grants No. PHY-0140324, No. INT-0115336, and No. PHY-0098793), the Department of Science and Technology, Government of India, the U.K. Science and Engineering Research Council, and the U.S. Department of Energy Nuclear Physics Division, under Contract No. W-31-109-ENG-38.

[1] S. Frauendorf, Rev. Mod. Phys. **73**, 463 (2001).
[2] S. Frauendorf and J. Meng, Nucl. Phys. **A617**, 131 (1997).
[3] C. M. Petrache *et al.*, Nucl. Phys. **A597**, 106 (1996).
[4] K. Starosta *et al.*, Phys. Rev. Lett. **86**, 971 (2001).
[5] A. A. Hecht *et al.*, Phys. Rev. C **63**, 051302(R) (2001).
[6] T. Koike, K. Starosta, C. J. Chiara, D. B. Fossan, and D. R. LaFosse, Phys. Rev. C **63**, 061304(R) (2001).
[7] D. J. Hartley *et al.*, Phys. Rev. C **64**, 031304(R) (2001).
[8] K. Starosta, T. Koike, C. J. Chiara, D. B. Fossan, and D. R. LaFosse, Nucl. Phys. **A682**, 375c (2001).
[9] C. W. Beausang *et al.*, Nucl. Phys. **A682**, 394c (2001).
[10] R. A. Bark, A. M. Baxter, A. P. Byrne, G. D. Dracoulis, T. Kibedi, T. R. McGoram, and S. M. Mullins, Nucl. Phys. **A691**, 577 (2001).
[11] K. Starosta, C. J. Chiara, D. B. Fossan, T. Koike, T. T. S. Kuo, and D. R. LaFosse, Phys. Rev. C **65**, 044328 (2002).
[12] I.-Y. Lee, Nucl. Phys. **A520**, 641c (1990).
[13] D. C. Radford, Nucl. Instrum. Methods Phys. Res., Sect. A **361**, 297 (1995).
[14] D. C. Radford, Nucl. Instrum. Methods Phys. Res., Sect. A **361**, 306 (1995).
[15] A. Krämer-Flecken, T. Morek, R. M. Lieder, W. Gast, G. Hebbinghaus, H. M. Jäger, and W. Urban, Nucl. Instrum. Methods Phys. Res., Sect. A **275**, 333 (1989).
[16] V. E. Iacob and G. Duchêne, Nucl. Instrum. Methods Phys. Res., Sect. A **399**, 57 (1997).
[17] W. F. Piel, Jr., C. W. Beausang, D. B. Fossan, L. Hildingsson, and E. S. Paul, Phys. Rev. C **35**, 959 (1987).
[18] E. M. Beck, F. S. Stephens, J. C. Bacelar, M. A. Deleplanque, R. M. Diamond, J. E. Draper, C. Duyar, and R. J. McDonald, Phys. Rev. Lett. **58**, 2182 (1987).
[19] S. Frauendorf, Nucl. Phys. **A557**, 259c (1993).
[20] S. Frauendorf, Z. Phys. A **358**, 163 (1997).
[21] S. Frauendorf, Nucl. Phys. **A677**, 115 (2000).
[22] V. I. Dimitrov, S. Frauendorf, and F. Dönau, Phys. Rev. Lett. **84**, 5732 (2000).
[23] V. I. Dimitrov, F. Dönau, and S. Frauendorf, Phys. Rev. C **62**, 024315 (2000).
[24] E. Mergel *et al.*, Eur. Phys. J. A **15**, 417 (2002).
[25] C. M. Petrache *et al.*, Phys. Rev. C **65**, 054324 (2002).